

A “simple” atom interferometry determination of G at 10^{-5} using a cold atomic fountain

G. Rosi¹

¹*Dipartimento di Fisica e Astronomia & LENS, Università di Firenze,
INFN Sezione di Firenze, via Sansone 1, I-50019 Sesto Fiorentino (FI), Italy*

(Dated: February 7, 2017)

In this paper we propose a novel experimental setup for measuring G with a relative accuracy of 10^{-5} using a standard cold atomic fountain. After an introduction about the measurement method, we are going to discuss in details the major sources of systematic errors, providing also information about the expected statistical uncertainty. In the end a brief discussion about the feasibility of G determination at the 10^{-6} level is also reported.

I. INTRODUCTION

The Newtonian gravity constant G can be considered as the Mt. Everest of precision measurement science [1]. After more than two centuries from the original determination performed by H. Cavendish, experiments based on torsion balance or torsion pendulum still provide the values with the lower degree of uncertainty (~ 20 ppm); unfortunately discrepancies of several standard deviations between independent measurements are still present [2, 3]. Cold atom interferometry has proven to be a powerful and alternative tool for measuring inertial forces [4], but up to now it has not been able to produce G values metrologically significant. One of the main systematic effects that limits the accuracy is due to the inherent difficulty to characterize and stabilize the ballistic trajectory of the atomic cloud during the interferometric sequence. To partially relax such parameter, a viable option is to employ a set of dense source masses to create stationary points along the vertical acceleration profile. In this case it is possible to identify a position \bar{z} of the atomic cloud apogee such as

$$\left. \frac{\partial \phi(z)}{\partial z} \right|_{\bar{z}} \simeq 0 \quad (1)$$

where ϕ is the interferometric phase shift. Thanks to this strategy, a G determination at 150 ppm level has been realized by Rosi et al. [5] using an ^{87}Rb cold atom gravity gradiometer, which consists of two vertically displaced, simultaneous Raman Mach-Zehnder interferometers. According to the error budget reported in [6], the systematic uncertainty on G due to an error of 0.1 mm on clouds vertical positions has to be evaluated to be 5 ppm, while the same error on the cloud vertical size produce a large shift of 56 ppm. Therefore, it appears evident that, in order to improve the accuracy of one order of magnitude, clouds dimensions must be contained in a $\sim \text{mm}^3$ of volume during the ballistic flight. In principle, this can be done using an ultra-cold atomic source [7]. However, having in mind the usual gradiometer scheme, it is technically challenging to produce a pair of ultra-cold samples and place them routinely with a spatial resolution below $100 \mu\text{m}$. At this scope, schemes based on interferometers

trapped in optical lattices has been proposed and experimentally demonstrated [8], but they have not yet reached the required maturity level for metrological applications.

A possible alternative way to overcome this kind of geometric limitations with an atomic gravity-gradiometer can be found following the method suggested in a recent work of A. Roura [9]. Here, it has been demonstrated that changing the k_{eff} vector of the Raman beam by a certain amount Δk_{eff} at the central π pulse of an usual interferometric sequence produces a phase shift equivalent to the one induced by a constant gravity gradient Γ_{ext} . In particular the following relation holds:

$$\Delta k_{\text{eff}} = (\Gamma_{\text{ext}} T^2 / 2) k_{\text{eff}} \quad (2)$$

where T is the free evolution time and d the distance between the atomic samples. Therefore, with a proper choice of Δk_{eff} we can compensate the effective gravity gradient Γ probed by the atoms. This matching condition can be easily found by determining experimentally the zero phase shift condition

$$\Phi = k_{\text{eff}}(\Gamma - \Gamma_{\text{ext}})dT^2 = 0 \quad (3)$$

which is valid regardless the value of d . This feature is fundamental to accomplish high precision equivalence principle tests with atoms in free fall but it is also useful to perform gravity gradient measurements less dependent from the clouds position. Strictly speaking, a geometry-free gradient determination can be realized when the probed acceleration profile is perfectly linear, or, more generally, if it is possible to find a condition where

$$\left. \frac{\partial \Gamma(z, d)}{\partial z} \right|_{\bar{z}, \bar{d}} = \left. \frac{\partial \Gamma(z, d)}{\partial d} \right|_{\bar{z}, \bar{d}} \simeq 0 \quad (4)$$

Clearly, when applied to a G determination, this relation completely changes the experimental strategy.

In the following section, an experimental scheme for an improved cold atom determination of the Newtonian constant is briefly described. In section III requirements in term of statistical uncertainty and sensitivity is reported, while in section IV we are going to quantitatively discuss

the main systematic effects. Finally, in section 5, conclusions and prospects for experimental determination towards 10^{-6} level are presented.

II. PRINCIPLE OF OPERATION

In figure 1 a sketch of the experimental apparatus is reported.

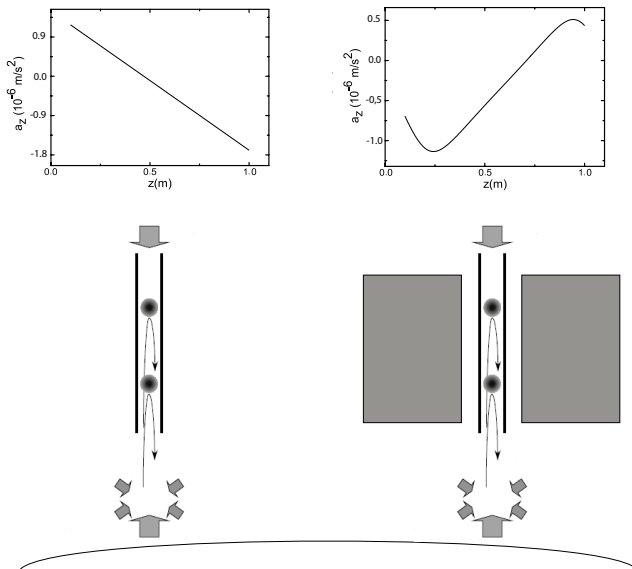


FIG. 1. Sketch of the experiment. Two atomic samples are trapped and cooled in a magneto-optical trap (MOT) and sequentially launched towards the interferometric region. A measurement of the local gravity gradient is performed by a Raman interferometry scheme. When local gravity anomalies are far enough (Far configuration, left side), the gravity acceleration profile given by the Earth is almost perfectly linear. The same condition can be also realized by using a proper shaped source mass that surrounds the atomic sensor (Close configuration, right side). The value of the gravity constant can be retrieved by measuring the corresponding modulation of the gravity gradient.

Here we consider a gravity gradiometer that consists in a pair of thermal clouds of ^{87}Rb launched from a MOT with standard moving molasses technique and simultaneously interrogated by a sequence of three counter-propagating Raman pulses. Comprehensive description of this well-established technologies can be found in literature [10, 11] and therefore we will not provide here any experimental details about them. The motivation of such instrument choice lies in the intention to keep the system as simple as possible. Further efforts to improve the atomic source may be spent to push the measurement below the 10^{-5} limit.

The basic idea is to modulate the value of the gravity gradient of the Earth (Figure 1, left side, “Far” configuration) with a properly designed source mass (Figure

1, right side, “Close” configuration). From the resulting gravity gradient variation $\Delta\Gamma$, evaluated with the zero phase shift technique, it will be possible to retrieve the value of G , in a similar way to what was done in [5].

Globally, Earth’s gravity gradient Γ_E is expected to be quite constant in function of the elevation h . According to the free-air correction formula, the second order coefficient is $\simeq h/R_T$ smaller than Γ_E , where R_T is the Earth’s radius [12]. Locally, the acceleration profile can be easily warped by nearby objects and local gravity anomalies. However we can roughly set a requirement on acceleration linearity according to our ability to control the atomic sample vertical coordinate z . Let us suppose to have a jittering $\delta z \simeq 1$ mm and to be in presence of a spherical anomaly (radius R , density contrast $\Delta\rho$) placed below the instrument at distance r . It can be easily found that

$$\frac{\delta\Gamma}{\Gamma_E} \simeq 5.4 \times 10^{-4} \Delta\rho \frac{R^3}{r^3} \frac{\delta z}{r} \quad (5)$$

imposing $\delta\Gamma/\Gamma_E = 10^{-5}$ and taking $\Delta\rho = 2 \times 10^3$ kg/m³, we can set some upper limits on the anomaly size. For instance, for $r = 1, 5, 10$ and 50 m we have $R = 0.2, 2, 4.5$ and 38.6 m, while $R \simeq r$ at $r = 100$ m. We can conclude that the apparatus must be placed sufficiently far from underground structures and aquifers, while regional scale anomalies can be ignored. A ground-based gravity survey can also help to carefully characterize the area. It is interesting to point out that the largest mass anomaly in the experiment could be represented by the source mass itself, which must be vertically displaced far enough from the interferometer area in order to actually realize the Far configuration.

In order to synthesize an additional linear gravity gradient to probe, a proper source mass geometry must be selected. Moreover, the shape should be as simple as possible, in order to simplify the machining process. A hollow cylinder produces along its vertical axis an acceleration profile with a good degree of linearity (see Figure 1, right part), once proper dimensions and material have been selected. In the following we are going to define such parameters, according to the requirements on statistical and systematic errors.

III. STATISTICS

As mentioned before, the key point of the method relies in determining the zero phase shift condition, at which corresponds, according to equation 2 and 3, a given frequency jump $\Delta\nu_0 = c\Delta k_{\text{eff},0}/4\pi$. A naive way to perform such operation is to measure two gradiometric phases $\Phi(\Delta\nu = 0)$ and $\Phi(\Delta\nu) \simeq -\Phi(0)$ for each source mass configuration. It is straightforward to see that

$$\Delta\nu_0 = \frac{\Phi(0)}{\Phi(0) - \Phi(\Delta\nu)} \Delta\nu \quad (6)$$

and

$$\frac{\delta(\Delta\nu_0)}{\Delta\nu_0} = \sqrt{\frac{(\delta\Phi)^2}{\Phi^2} + \frac{2(\delta\Phi)^2}{(\Phi(0) - \Phi(\Delta\nu))^2} + \frac{(\delta\Delta\nu)^2}{\Delta\nu^2}} \quad (7)$$

$$\simeq \frac{\sqrt{2}\delta\Phi}{\Phi(0)}$$

The $\delta(\Delta\nu)/\Delta\nu$ term can be neglected since the Raman lasers frequency can be set with a very high degree of precision and stability. Therefore, we can roughly estimate the statical error on G as

$$\left(\frac{\delta G}{G}\right)_{stat} = \frac{2\delta\Phi}{\Phi(0)^C - \Phi(0)^F} = \frac{2\delta\Phi}{k_{eff}(\Delta\Gamma)dT^2} \quad (8)$$

In this expression all the relevant experimental parameters are contained: the effective signal $\Delta\Gamma$ is determined by the density of the source mass while its linear dimension is set by d and T . Considering tungsten alloy as source mass material ($\Delta\Gamma \simeq 2\Gamma_E$), using standard Raman optics and taking $T = 0.243$ s and $d = 0.29$ m, we obtain $\delta\Phi = 8$ μ rad for 10 ppm on G . For comparison, in [5], the corresponding $\delta\Phi$ value was 44 μ rad after 100 hours of integration. To cover such factor 5 gap without dramatically increase the size of the apparatus and/or the integration time, at least two solutions are, in principle, possible. Enhancing k_{eff} using multi-photon pulses is the most evident one but unfortunately, at least for thermal clouds, several factors limiting the contrast for large T are present, in addition to the impossibility to have a convenient internal state mapping [13]. For Rb, and in general for Alkali, one could make use of Raman transitions acting on the $5S \rightarrow 6P$ manifold. In this case, with $\lambda = 422$ nm, a small but metrologically significant gain in sensitivity of 1.8 is ensured. Finally, as it will be shown in the next section, one of the strong point of the presented setup lies in the small systematic contribution due to the cloud atomic size and temperature. As a consequence, atomic flux can be increased by a factor of ten or even more, for example by relaxing the selectivity in velocity and implementing $m_F = 0$ optical pumping.

IV. SYSTEMATICS

In precision measurements, and in particular for a G determinations, keep under control systematic shifts is by far the more demanding task. It is beyond the scope of this work to perform a full *a priori* evaluation of each possible error source. We will focus our attention mostly on the effects produced by the finite dimension of our atomic probe, in order to put in evidence the most interesting features of the method. Nevertheless, prior to address this topic, it is worth to discuss some basic criteria regarding the source mass design. In the following we will consider a monolithic hollow cylinder in order to

simplify the discussion. If necessary, an almost equivalent geometry can be realized using smaller cylinders radially arranged, as it was done in [14].

A. Source Mass

The vertical acceleration profile $a(z)$ along the axis of an hollow cylinder having a homogeneous density ρ , a height H , and an inner and outer radius R_1 and R_2 can be analytically calculated [15]:

$$a(z) = 2\pi\rho G(r_{2-} - r_{2+} + r_{1+} - r_{1-}) \quad (9)$$

$$r_{i\pm} = \sqrt{R_i^2 + \left(\frac{1}{2}H \pm z\right)^2}, \quad i = 1, 2.$$

As explained before, the value of H is roughly defined by the gradiometry vertical extension while R_1 and R_2 should be chosen in order to produce an acceleration profile with a good degree of linearity. At this scope it is convenient to develop in series the previous equation:

$$\frac{a(z)}{2\pi\rho G} = H \left(\frac{1}{\sqrt{H^2/4 + R_1^2}} - \frac{1}{\sqrt{H^2/4 + R_2^2}} \right) z$$

$$+ \frac{H}{2} \left(\frac{R_2^2}{(H^2/4 + R_2^2)^{2.5}} - \frac{R_1^2}{(H^2/4 + R_1^2)^{2.5}} \right) z^3 \quad (10)$$

$$+ \dots$$

Here it is possible to identify several (R_2, R_1) couples that conveniently cancel the cubic term.

Remarkably, it comes out that having the cubic component small or equal to zero also lead to a reduced sensitivity with respect to the radial coordinate r . Indeed, according to [15], it can be demonstrated that the second derivative of the acceleration with respect to r is 1/2 times the second derivative of the acceleration with respect to z . As a consequence, the advantage of working in the linear region of $a(z)$ rather than in the stationary points is twofold.

Having this in mind and keeping into account limits due to apparatus size, we can determine suitable test values for the hollow cylinder; in our case, considering the interferometer parameters described in the previous section, we choose $R_2 = 0.556$ m, $R_1 = 0.120$ m and $H = 0.770$ m. Selecting such large dimensions not only helps in keeping a good S/N ratio but also in relaxing the required accuracy in shape. From equation 3 we estimate that an uncertainty of 10 μ m on height or diameters already produces a systematic shift on G of 10 ppm. A size reduction of a factor 2 or 3 can only worsen the situation. Regarding the material, possible options are lead, tungsten alloy and mercury. The latter is the best one in term of homogeneity, but its huge thermal expansion coefficient (61×10^{-6} K $^{-1}$) require a temperature stabilization better than 100 mK. Lead is the cheapest one,

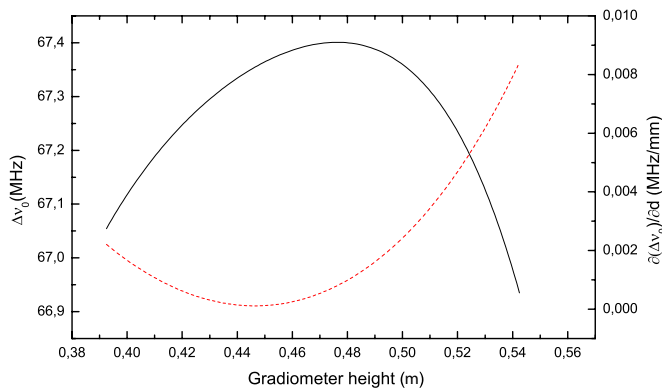


FIG. 2. Black solid line: plot of the simulated zero shift frequency jump $\Delta\nu_0$ versus the gradiometer height z , defined as the average between the apogee points. Dashed red line: plot of the corresponding d punctual derivative, where d is the vertical distance between interferometers. Source mass lower surface is placed at $z = 0$

but also the less dense and the most difficult to machine. Tungsten alloy can be shaped with a micrometric precision and its high density ($\rho = 18000 \text{ Kg/m}^3$) is ideal to induce a high gravity gradient. Choosing this latter, the total mass of the hollow cylinder amounts to 13 tons. It is worth to point out that such kind of number are not new in the field of the G metrology [16].

B. Atomic trajectories

Now that the relevant source mass features has been defined, an evaluation of the expected shifts due to the atomic clouds size can be performed. The first step is to optimize the atomic trajectory along the vertical axis of the system. In Figure 2 the expected $\Delta\nu_0$ value is plotted versus the gradiometer height z , defined as the average of the apogee vertical coordinates. In addition also the quantity $\partial(\Delta\nu_0)/\partial d$ has been punctually evaluated in function of z . A single particle simulation has been employed, using the interferometer parameters defined in section II. We notice that $\Delta\nu_0$ cannot be stationary for z and d simultaneously. We choose to fix z such as $\partial(\Delta\nu_0)/\partial z = 0$ mainly because d is easily and accurately measured during the G measurement and therefore less critical. Since all the single particle parameters have been determined, a Montecarlo simulation can be carried out. To estimate the uncertainty on G measurement, derivatives with respect to the relevant clouds parameters have been computed. The results are summarized in table I.

Even if, compared to [5], the selected uncertainties are equal or twice larger, the total systematic error remains

below 10 ppm. As expected, the sensitivity with respect to the vertical coordinates is considerably suppressed. This can also be seen from the point of view of the mass positioning: an error of 5 mm induces a total shift of only 2 ppm. Therefore there is no need of micrometric translation stages and optical rulers, a valuable opportunity when a heavy object must be translated over a long distance ($\sim 4 \text{ m}$ for far configuration). Also radially, the overall G dependency is reduced by a factor ~ 10 , much more than expected from the simple scaling factor of the apparatus.

C. Other effects

Approaching the 10 ppm accuracy requires attention also to other parameters that did not constitute a limit in previous determination. The most problematic, especially for a cold atomic fountain, is the Coriolis shift, which is always present in a free-fall interferometer. Compensation schemes based on counteracting the the Earths rotation rate by acting on the retroreflecting Raman mirror [17, 18] must be optimized towards the percent accuracy. Of course, the source mass movement system must be well isolated from the fountain holding structure in order to avoid spurious tilts. Also magnetic fields must be kept under control along the interferometer region. An accurate design of the magnetic shields and the bias coils surrounding the interferometer tube is crucial. However, it is worth to remember that modulating the signal by periodically switching between source mass configurations and reversing the k_{eff} vector [19] is a powerful strategy to suppress this kind of shifts.

V. CONCLUSIONS AND PROSPECTS

In this paper a preliminary study about a G determination at 10 ppm using a cold atom fountain is reported. With a proper implementation of the method described in [9], systematic effects due to the clouds size, temperature and trajectories are genuinely suppressed. In order to push the accuracy towards the 10^{-6} , the implementation of ultra-cold atomic sources and large momentum transfer atom optics helps a lot in order to enhance short term sensitivity and optimize the control over systematic shifts. If spurious magnetic fields represents the ultimate accuracy limit, using ^{88}Sr instead of Rb should be a viable option [20]. However, it is likely that main issues might come from the source mass itself. In this case shape characterization below $1 \mu\text{m}$ seems unavoidable and the material inhomogeneities could be really hard to characterize.

TABLE I. Atomic cloud parameters, corresponding uncertainties and simulated relative shifts on G . Uncertainties are quoted as one standard deviation.

Parameter	Uncertainty in parameter	Relative uncertainty on G (ppm)
Baricenters height	1 mm	< 1
Baricenters vertical distance	0.2 mm	2.6
Baricenters radial position	2 mm	< 1
Baricenters radial velocity	2 mm/s	< 1
Clouds vertical size	0.3 mm	1.7
Clouds horizontal size	0.5 mm	2.8
Clouds vertical expansion	0.3 mm/s	< 1
Clouds transversal expansion	2 mm/s	4.2
Total		6.0

- [3] H. V. Parks and J. E. Faller, Phys. Rev. Lett. **105**, 110801 (2010)
- [4] *Atom Interferometry, Proceedings of the International School of Physics Enrico Fermi, Course CLXXXVIII*, edited by G. M. Tino and M. A. Kasevich (Società Italiana di Fisica and IOS Press, Amsterdam)(2014)
- [5] G. Rosi, F. Sorrentino, L. Cacciapuoti, M. Prevedelli, and G. M. Tino, Nature **510**, 518521 (2014)
- [6] M. Prevedelli, L. Cacciapuoti, G. Rosi, F. Sorrentino, and G. M. Tino, Phil. Trans. R. Soc. A **372**, 2026 (2014)
- [7] T. Kovachy, P. Asenbaum, C. Overstreet, C. A. Donnell, S. M. Dickerson, A. Sugarbaker, J. M. Hogan, and M. A. Kasevich, Nature **528**, 530533 (2015)
- [8] X. Zhang, R. D. Aguila, T. Mazzoni, N. Poli, and G. M. Tino, Phys. Rev. A **94**, 043608 (2016)
- [9] A. Roura, arXiv:1509.08098(2015)
- [10] J. M. McGuirk, G. T. Foster, J. B. Fixler, M. J. Snadden, and M. A. Kasevich, Phys. Rev. A **65**, 033608 (2002)
- [11] F. Sorrentino, Q. Bodart, L. Cacciapuoti, Y.-H. Lien, M. Prevedelli, G. Rosi, L. Salvi, and G. M. Tino, Phys. Rev. A **89**, 023607 (2014)
- [12] R. I. Hackney and W. E. Featherstone, Geophysical Journal **154**, 35 (2003)
- [13] G. D'Amico, F. Borselli, L. Cacciapuoti, M. Prevedelli, G. Rosi, F. Sorrentino, and G. M. Tino, Phys. Rev. A **93**, 063628 (2016)
- [14] G. Lamporesi, A. Bertoldi, A. Cecchetti, B. Dulach, M. Fattori, A. Malengo, S. Pettoruso, M. Prevedelli, and G. M. Tino, Rev. Sci. Instrum. **78**, 075109 (2007)
- [15] R. I. Hackney and W. E. Featherstone, Physics Letters A **248**, 295 (1998)
- [16] S. Schlamminger, E. Holzschuh, F. N. W. Kündig, R. E. Pixley, J. Schurr, and U. Straumann, Phys. Rev. D **74**, 082001 (2006)
- [17] J. M. Hogan, D. M. S. Johnson, and M. A. Kasevich, in *Proceedings of the International School of Physics Enrico Fermi Course CLXVIII on Atom Optics and Space Physics*, edited by E. Arimondo, W. Ertmer, W. P. Schleich, and E. M. Rasel (IOS Press, Amsterdam and SIF, Bologna), p. 411.(2007)
- [18] S.-Y. Lan, P.-C. Kuan, B. Estey, P. Haslinger, and H. Müller, Phys. Rev. Lett. **108**, 090402 (2012)
- [19] A. Louchet-Chauvet, T. Farah, Q. Bodart, A. Clairon, A. Landragin, S. Merlet, and F. P. D. Santos, New Journal of Physics **13**, no. 6, 065025 (2011)
- [20] T. Mazzoni, X. Zhang, R. D. Aguila, L. Salvi, N. Poli, and G. M. Tino, Phys. Rev. A **92**, 053619 (2015)